Chinese Journal of Catalysis 37 (2016) 1982–1990

available at www.sciencedirect.com

ScienceDirect

journal homepage: www.elsevier.com/locate/chnjc

Article

# Oxidation of glycerol with $H_2O_2$ on Pb-promoted Pd/γ-$Al_2O_3$ catalysts

María L. Faroppa [a], Juan J. Musci [a,#], María E. Chiosso [a,b], Claudia G. Caggiano [a], Hernán P. Bideberripe [b,c], José L. García Fierro [d], Guillermo J. Siri [b,c], Mónica L. Casella [a,b,*]

[a] *CIBA (CIT UNNOBA, CONICET), Universidad Nacional del Noroeste de la Provincia de Buenos Aires, Newbery 261 (6000) Junín, Provincia de Buenos Aires, Argentina*

[b] *CINDECA (CCT La Plata-CONICET, UNLP), Universidad Nacional de La Plata, Facultad de Ciencias Exactas, 47 N°257, 1900 La Plata, Argentina*

[c] *PIDCAT Facultad de Ingeniería, Universidad Nacional de La Plata, 1 y 47, 1900 La Plata, Argentina*

[d] *Instituto de Catálisis y Petroleoquímica, CSIC, Canto Blanco, E-28049 Madrid, España*

ARTICLE INFO

*Article history:*
Received 1 June 2016
Accepted 20 August 2016
Published 5 November 2016

*Keywords:*
Palladium
Bimetallic palladium-lead catalyst
Hydrogen peroxide
Glycerol oxidation
Glyceric acid
Glycolic acid

ABSTRACT

A series of bimetallic Pd-Pb catalysts with a constant Pd content of 1 wt% and Pb/Pd atomic ratio from 0 to 1.6 supported on γ-$Al_2O_3$ were prepared and used for glycerol oxidation with $H_2O_2$ as the oxidizing agent at atmospheric pressure, 45 °C and pH = 11. The morphology and dispersion of the catalysts were characterized by scanning electron microscopy-energy dispersive X-ray spectroscopy (SEM-EDX) and transmission electron microscopy (TEM). The presence of an alloy phase in the bimetallic catalyst was detected by X-ray photoelectron spectroscopy (XPS). Glycerol conversion obtained with the monometallic Pd catalyst was 19%, which was increased to 100% with the addition of Pb. The four bimetallic PdPb catalysts were able to oxidize glycerol to dihydroxyacetone (DIHA) and the selectivity to DIHA reached 59%, 58%, 34% and 25% for PdPb0.25, PdPb0.50, PdPb1.00 and PdPb1.60 catalysts, respectively.



## 1. Introduction

Glycerol is a compound with many functions, which provides the possibility of using it for the synthesis of many value-added chemical products. It has the further advantage that it is a nontoxic, edible, biosustainable and biodegradable compound [1]. In recent years, the catalytic conversion of glycerol to chemicals and fuels by reactions such as oxidation, hydrogenolysis, dehydration, pyrolysis-gasification, etherification, esterification and polymerization has been proposed in the literature [2].

In particular, the oxidation of glycerol leads to a complex network of reactions in which a large number of products such as dihydroxyacetone (DIHA), glyceric acid (GLYA), glycolic acid (GLYCA), oxalic acid (OXALA) and tartronic acid (TARAC) are obtained (Scheme 1) [3]. Many of these products are useful intermediate substances or valuable fine chemicals. For instance, glycolic acid is among the most popular functional ingredients in anti-ageing formulations. These products are currently synthesized by very expensive or complicated chemical processes or via biotechnology [4–8].

The oxidation of alcohols to obtain aldehydes, ketones and

* Corresponding author. Tel: +542214210711; E-mail: casella@quimica.unlp.edu.ar
# Becario de estudio orientado CIC PBA.
This work was supported by CONICET (PIP 0276), UNLP (Projects X 700), UNNOBA (SIB 2924/14), and Ministry of Education and Sports (Call "Jorge Sábato" Project 44-144-415), Argentina.
DOI: 10.1016/S1872-2067(16)62531-7 | http://www.sciencedirect.com/science/journal/18722067 | Chin. J. Catal., Vol. 37, No. 11, November 2016

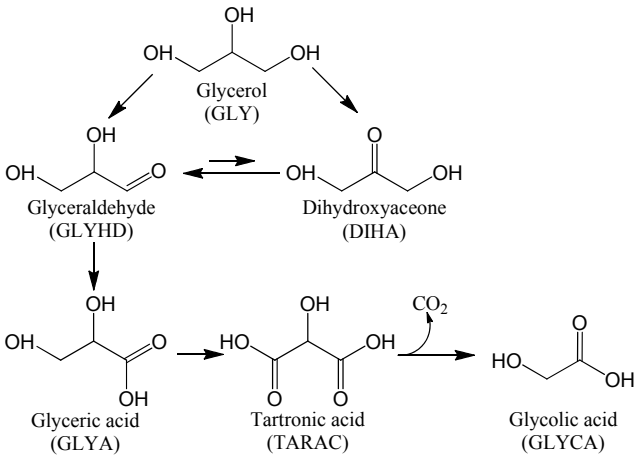


**Scheme 1.** Reaction pathways for the selective oxidation of glycerol.

carboxylic acids is one of the pivotal functional group transformations in organic chemistry. This process has traditionally been carried out using potassium dichromate solution acidified with dilute sulfuric acid. However, the use of these inorganic reagents in stoichiometric proportions is being displaced by new, more environmentally benign methods. The heterogeneous catalytic oxidation of glycerol is an environmentally friendly alternative to obtain one or more of its oxidation products [9]. Over the last ten years, the liquid phase oxidation of biomass-derived oxygenated compounds such as glycerol has been mainly studied on Au, Pt and Pd-based supported catalysts [10,11]. This process provides an opportunity to generate high value-added products with good selectivity under mild experimental conditions. However, there are still some practical problems in the utilization of these catalysts regarding their catalytic activity and deactivation [12].

Particular attention has been paid to the use of gold catalysts. Several authors have shown that supported gold catalysts are active and selective for the oxidation of the primary alcohol [13 and references therein]. With regard to the oxidation of glycerol, it has been reported that this reaction is structure sensitive since the catalytic activity and selectivity are strongly influenced by the size of the gold particles and the preparation method [14].

Regarding Pt and Pd-based catalysts, they are the most versatile in terms of their use in organic synthesis, and they have been reported to be highly active in the oxidation of alcohols. Several reports can be found in the literature indicating that the activity of Pt and Pd-based systems is strongly dependent on the pH at which the reaction is performed, and that even undesirable products such as carbon dioxide, formaldehyde and formic acid may be generated [15–17].

It has been suggested that the addition of a second metal (less active) such as Bi, Pb or Sn to Pt or Pd catalysts can lead to an improvement in their catalytic performance. Nevertheless, the actual origin of the function of the second metal added as the promoter of the noble metal and the probable benefit to the catalytic activity of the Pt or Pd-based systems remain a matter of debate [18,19].

The present paper describes experiments carried out to improve the understanding of the promoting role of Pb in alumina-supported Pd catalysts. The optimal Pb/Pd composition of the active phases was also investigated. The catalysts were characterized by transmission electron microscopy (TEM), temperature programmed reduction (TPR) and X-ray photoelectron spectroscopy (XPS). Their activity and selectivity in the aqueous phase oxidation of glycerol were evaluated using $H_2O_2$ as oxidizing agent. When considering the oxidation of glycerol using supported palladium catalysts, the pH is an aspect that influences both the catalytic activity and selectivity. By tuning the reaction pH, one can direct the oxidation to different product profiles. For that reason, in the present paper, alkaline conditions were selected to study the glycerol oxidation reaction.

## 2. Experimental

### 2.1. Preparation of catalyst

The 1 wt% Pd/γ-$Al_2O_3$ catalyst was prepared by ion exchange with an aqueous solution of $PdCl_2$ (Aldrich). The mass of $PdCl_2$ needed for 1wt% Pd in the final catalyst was dissolved in a HCl solution (0.01 mol/L) to generate a water-soluble palladium chloro-complex. The γ-$Al_2O_3$ used as support (Air Products and Chemical & Gas SRL, $S_{BET}$ = 180 $m^2/g$) was left in contact with the palladium solution for 24 h, after which the liquid was separated by decantation and the solid was dried in an oven at 105 °C for 24 h. The reduction of palladium was performed by adding a solution of formaldehyde (37 wt%), and then a KOH solution (30 wt%). To do this, the palladium catalyst was placed in an Erlenmeyer flask that was immersed in a water bath at 50 °C and formaldehyde solution was added dropwise until the catalyst turned to dark gray. Then, KOH solution was added to reach a pH value between 9.5 and 10.0. Finally, it was heated in an oven at 60 °C for 24 h.

Before proceeding to the impregnation of lead, the chloride present in the catalyst was eliminated. To do this, the solid was washed with distilled water until there was no chloride as verified with silver nitrate.

Pb-modified Pd/γ-$Al_2O_3$ catalysts were prepared by impregnation with $Pb(NO_3)_2$ (Cicarelli). Four bimetallic catalysts were prepared whose Pb/Pd atomic ratios were 0.25, 0.50, 1.00 and 1.60. In each preparation, a calculated amount of lead nitrate was weighed and dissolved in 5 mL of distilled water. This solution was added to the monometallic catalyst. The system was left in contact for 24 h and then was heated in an oven at 105 °C for 24 h. Before use, each catalyst was reduced in a hydrogen flow for 2 h at 300 °C. These catalysts were designated PdPb0.25, PdPb0.50, PdPb1.00 and PdPb1.60.

### 2.2. Catalyst characterization

The concentrations of Pd and Pb in the catalysts were measured by atomic absorption spectroscopy using a Varian 240 AA spectrophotometer after dissolving the solid. The catalysts were analyzed by TPR using 50 mg of catalyst, 5% $H_2$ in Ar at a flow rate of 7.3 mL/min and a heating rate of 10 °C/min from room temperature to 800 °C. $H_2$ consumption during re-

duction was analyzed online with a Shimadzu GC-8A gas chromatograph with a thermal conductivity detector (TCD).

scanning electron microscopy/energy dispersive X-ray spectroscopy (SEM/EDX) measurements were performed using a FEI Quanta 200 SEM equipped with EDX (EDX SDD Apollo 40). In order to draw conclusions about the distribution of the components in the samples, images of back scattered electrons (BSE) were taken.

The size distribution of the metal particles was determined by TEM using a JEOL 100 CX instrument. Samples were ground and ultrasonically dispersed in distilled water. For the determination of the particle size distribution histograms, over 200 Pd particles were measured from the micrographs taken directly from the screen using the bright field image. The mean particle diameter ($d_{TEM}$) was calculated using the formula:

$$d_{TEM} = \frac{\sum_i n_i d_i^3}{\sum_i n_i d_i^2}$$

where $n_i$ is the number of particles of diameter $d_i$.

XPS analysis was performed on a Shimadzu ESCA 750 instrument equipped with a Mg $K_\alpha$ (1253.6 eV) X-ray source and a hemispherical analyzer. The fresh sample was placed on an accessory that allowed its transfer from the pretreatment chamber to the analysis chamber. The sample was reduced *in situ* at 300 °C for 1 h. The carbon 1*s* impurity line at 284.6 eV was used for binding energy (BE) calibration.

### 2.3. Oxidation experiments

The aqueous phase oxidation of glycerol (0.3 mol/L) was carried out at atmospheric pressure in a 250 mL glass reactor with constant stirring and immersed in a thermostatic bath that kept the temperature inside the reactor at 45 °C. In a typical test, 100 mg of catalyst was used and $H_2O_2$ 5 vol% as oxidizing agent. At the beginning of the reaction, NaOH was added to give a pH = 11. Zero time was taken as just before the addition of the catalyst into the reactor. The reaction conditions for the catalytic tests were chosen so that the reaction rate was not influenced by mass transfer.

Periodically, samples were taken from the reactor and analyzed by liquid chromatography (HPLC) using a UHPLC DIONEX UltiMate 3000 equipment with a UV detector (210 nm) and refractive index (RI) detector in series. The separation of the compounds was carried out on a PhenoSphere 5μ Sax 80 A (250 mm × 4.6 mm) ion exclusion column at 25 °C. The eluent was 5 mmol/L $H_2SO_4$ (0.6 mL/min). The products were identified by comparison with pure standards (Sigma Aldrich).

The conversion was determined by monitoring the concentration of glycerol as a function of time:

$$x_{Gly} = \frac{M^0_{Gly} - M^t_{Gly}}{M^0_{Gly}}$$

where $x_{Gly}$ is the conversion of glycerol, $M_{Gly}{}^0$ is the initial molar concentration of glycerol, and $M_{Gly}{}^t$ is the molar concentration of glycerol at time *t*. Initial reaction rates were calculated from the slopes of the curves of glycerol conversion (measured at reaction time corresponding to 10% conversion) by the following equation:

$$r_i = \frac{\text{Glycerol (mol)}}{\text{Reaction time (s)} \times \text{Pd (g)}}$$

According to reference [20], the selectivity of compound *i* ($S_i$) was calculated using the following equation:

$$S_i = \frac{M_i^t}{\left(M^0_{Gly} - M^t_{Gly}\right)} \cdot \frac{n_i}{3}$$

where $M_i{}^t$ is the molar concentration of compound *i* at time *t*, and $n_i$ is the number of carbon atoms of compound *i*.

## 3. Results and discussion

### 3.1. Preparation and characterization of the catalysts

Table 1 shows the results of the chemical composition of the catalysts determined by atomic absorption spectroscopy.

SEM/EDX analysis was performed to investigate the morphological characteristics of the catalysts. Fig. 1 depicts the SEM micrograph of the Pd/γ-$Al_2O_3$ catalyst. The porous structure characteristic of the γ-$Al_2O_3$ support was observed. The density and distribution of Pd on this sample were evaluated by EDX. Pd was uniformly distributed on the entire surface of the catalyst, as seen for instance, in E1, whose spectrum is shown in the inset of Fig. 1.

Fig. 2 shows SEM images of the analyzed bimetallic catalysts. In all cases, the porous morphology of the support was observed, as well as some individual and separated granules on its surface (which appeared as bright spots in the micrographs)

**Table 1**
Chemical composition and mean particle size measured by TEM for the catalysts.

| Catalyst | Pd (wt%) | Pb (wt%) | Pb/Pd (at/at) | $d_{TEM}$ (nm) |
|---|---|---|---|---|
| Pd/γ-$Al_2O_3$ | 0.98 | — | — | 7.2 |
| PdPb0.25 | 0.98 | 0.50 | 0.25 | 7.9 |
| PdPb0.50 | 0.98 | 0.94 | 0.50 | 7.7 |
| PdPb1.00 | 0.98 | 2.01 | 1.00 | 7.2 |
| PdPb1.60 | 0.98 | 2.87 | 1.60 | 7.3 |

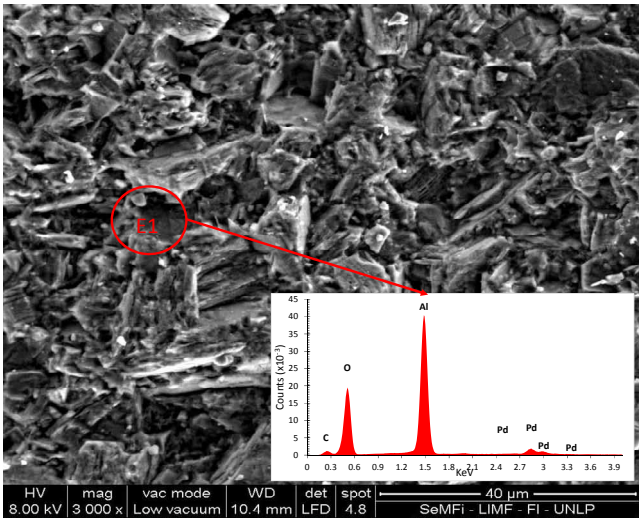


**Fig. 1.** SEM micrograph of the Pd/γ-$Al_2O_3$ catalyst showing a representative EDX spectrum taken at point E1 in the inset.

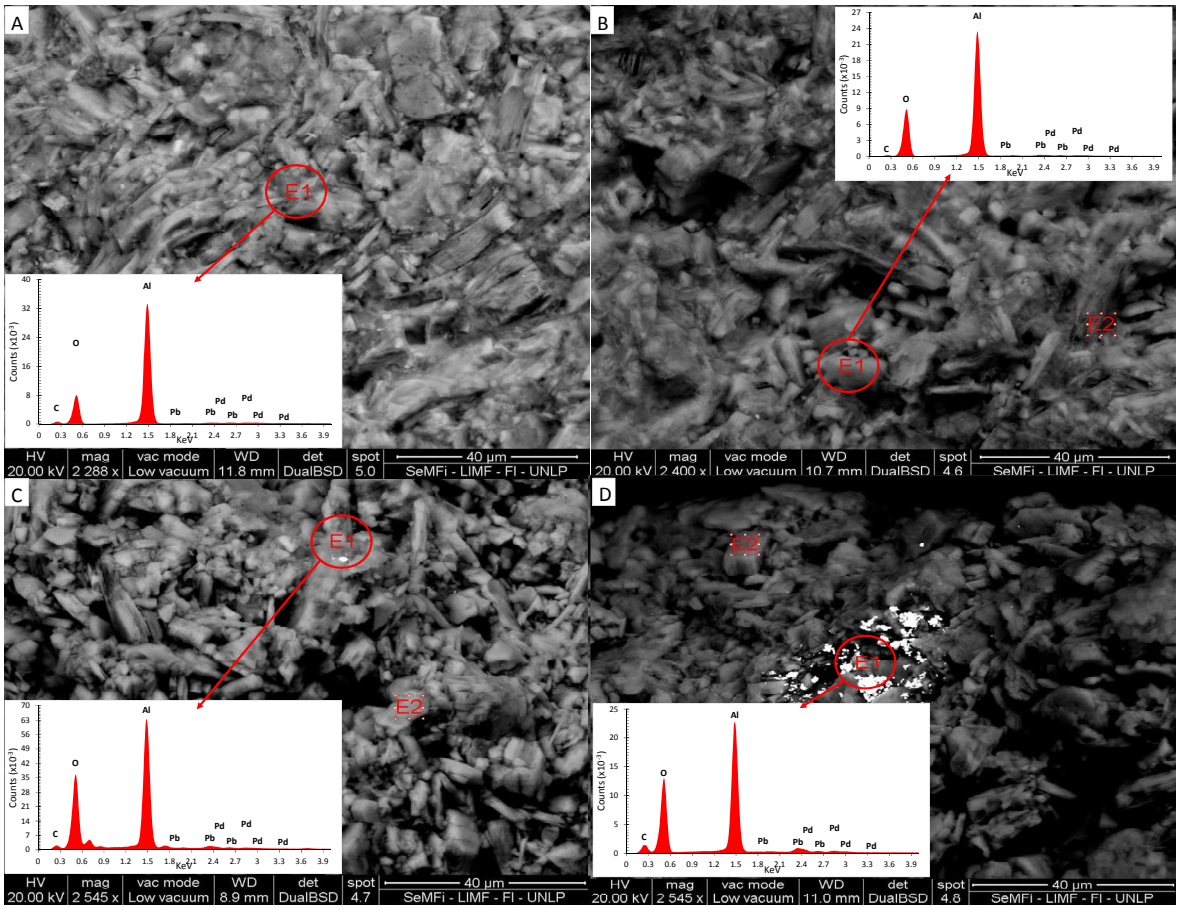


**Fig. 2.** SEM micrographs, and EDX spectra taken at E1 points of PdPb0.25 (A), PdPb0.50 (B), PdPb1.00 (C), and PdPb1.60 (D).

corresponding to lead. In each image, a point was selected (designated as E1) at which the EDX spectrum was taken. As shown in each of the insets, Pd and Pb always appear very close to each other, indicating that the preparation method was adequate and allowed an effective deposit of lead on palladium.

The Pd particle size and distribution of the catalysts were further characterized by TEM. Fig. 3 displays a TEM image of the monometallic catalyst, and Fig. 4 shows the representative micrographs of the four bimetallic catalysts.

The histograms of particle size distribution calculated from the micrographs are shown in the lower right corner of the TEM images. From the analysis of the data, it can be seen that the addition of lead hardly affected the particle size relative to the monometallic system. This would be an indication of the interaction between the two metals.

Fig. 5 illustrates the TPR diagrams of the catalysts. The monometallic $Pd/Al_2O_3$ sample exhibited a negative peak at 50 °C, associated with palladium β-hydride decomposition evolving hydrogen from the sample [21]. The appearance of this peak agreed with a fact well established in the literature that the β-hydride phase is only observed on Pd metal particles of appreciable size, as in the case of those measured by TEM [22]. Besides, a broad reduction signal in the 65–120 °C temperature range was observed, which was assigned to the reduction of $Pd^{2+}$ to metallic Pd [23].

Regarding the bimetallic PdPb catalysts, it is observed in Fig. 5 that the catalysts having a lower Pb content (PdPb0.25, PdPb0.50 and PdPb1.00) presented the negative peak associated with the decomposition of palladium hydride. The size of this peak decreased as the amount of lead increased, which was ascribed to an "isolation site effect" exerted by Pb on Pd. As mentioned in the previous paragraph, smaller Pd particles ab-

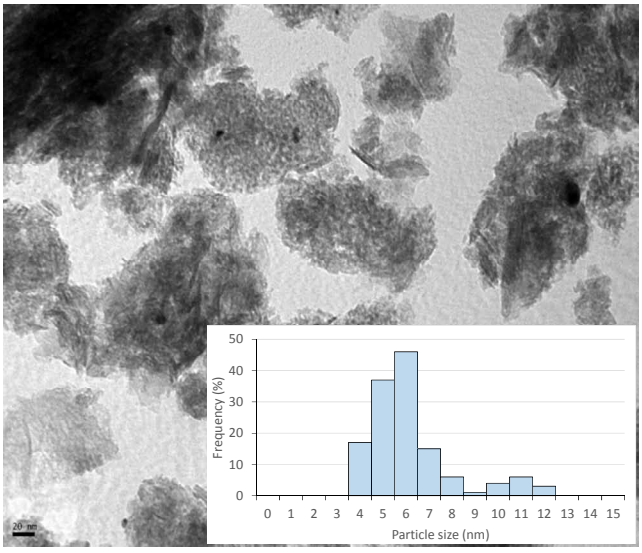


**Fig. 3.** TEM image of $Pd/\gamma\text{-}Al_2O_3$ catalyst and its particle size distribution histogram in the inset.

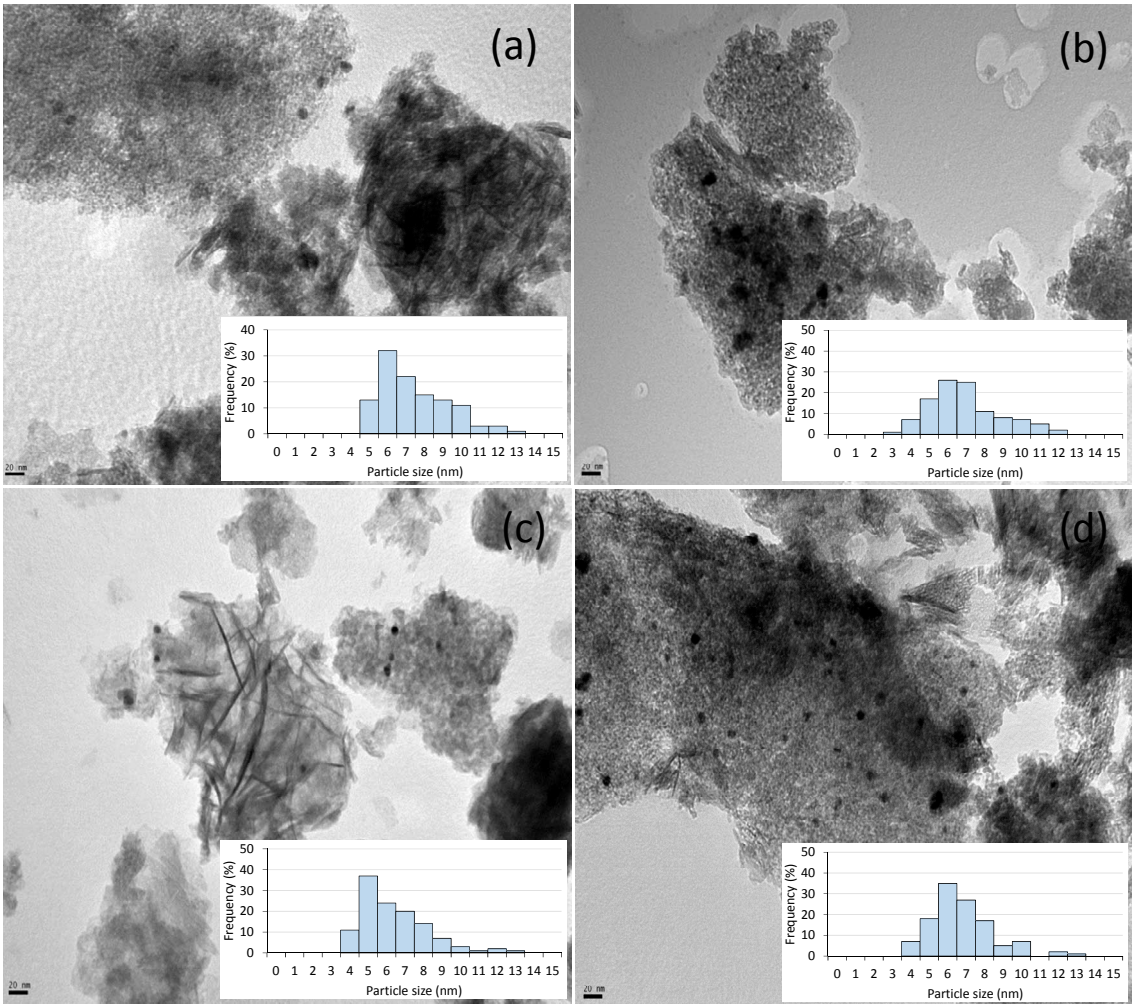


**Fig. 4.** TEM images of alumina supported bimetallic catalysts. (a) PdPb0.25; (b) PdPb0.50; (c) PdPb1.00; (d) PdPb1.60. The insets show their particle size distribution histograms.

sorb less hydrogen in the β-hydride phase than the larger ones. The catalyst with the highest lead content (PdPb1.60) did not show the negative peak of hydrogen evolution. All the bimetallic catalysts exhibited a large peak between 60 and 120 °C corresponding to the reduction of $Pd^{2+}$ to $Pd^0$.

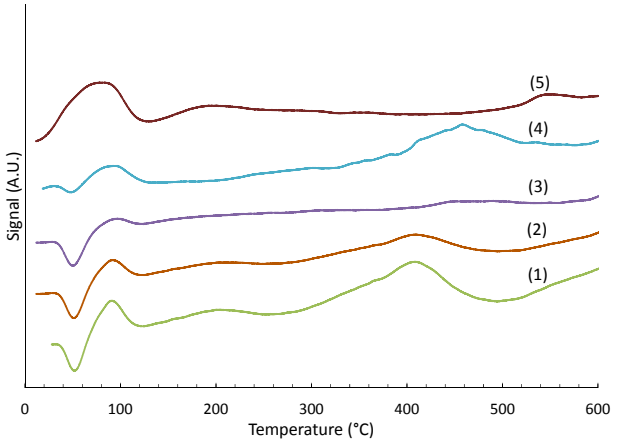


**Fig. 5.** TPR profiles of Pd/γ-$Al_2O_3$ (1), PdPb0.25 (2), PdPb0.50 (3), PdPb1.00 (4), and PdPb1.60 (5) catalysts.

In Fig. 6(a) and (b), the XPS results for Pd, PdPb0.25, PdPb0.50, PdPb1.00 and PdPb1.60 catalysts are presented. Table 2 summarizes the position of the main peaks relative to Al 2*p* at 74.5 eV. For the monometallic catalyst (Fig. 6(a)), the Pd $3d_{5/2}$ peak at 335.0 eV indicated that palladium was in the reduced state after the chemical reduction treatment. When the bimetallic catalysts were analyzed, a slight positive shift of 0.2 eV in the Pd $3d_{5/2}$ binding energy was observed. Although the value of this shift is within the error of the method, it may be assigned to an intermetallic compound according to the literature [24]. It is well documented in the literature that a correlation existed between the binding energy of palladium and the metal particle size [25]. According to the work of Bertolini *et al.* [26] Pd particles having a diameter larger than 2.8 nm present a BE value typical of bulk Pd. From the TEM measurements, the average particle size of all the Pd catalysts studied here was around 7.5 nm (Table 1) and correspondingly the BE values obtained from the XPS analysis were very close to that of bulk Pd.

Another remarkable result from the XPS measurements is the presence of between 20% and 30% of Pb in a reduced form (Fig. 6(b) and Table 2). Palladium forms a wide range of solid

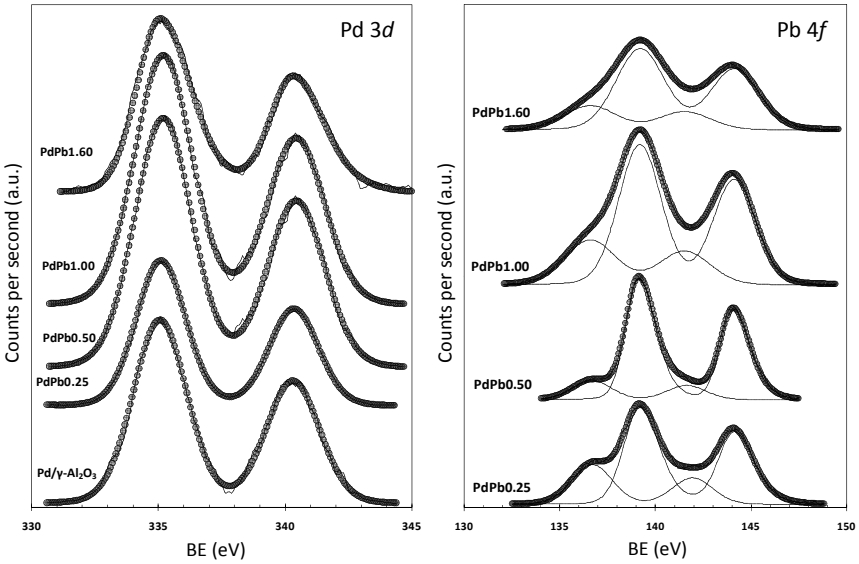


**Fig. 6.** XPS spectra of the catalysts in the Pd 3*d* region and Pb 4*f* region.

solutions with 10–30 wt% of low melting metals such as lead, so probably lead in the metallic state can be alloyed with Pd. Finally, among the bimetallic catalysts, PdPb0.50 presented a Pd $3d_{5/2}$/Al 2*p* atomic ratio (estimated from the relative intensities in Table 2) significantly lower than the other bimetallic catalysts. This fact could indicate that Pd particles were partially covered by Pb, and thus provided evidence of a close interaction between the both metals, in agreement with the TPR results [24].

### 3.2. Catalytic activity

In order to avoid mass transfer limitation, the liquid phase glycerol oxidation reaction was carried out at a stirring rate of 500 r/min, which was selected according to the literature [27]. The effect of $H_2O_2$ concentration was analyzed using three different concentrations (2.5, 5.0 and 10.0 active oxygen volume), while the other reaction parameters were kept constant. In Fig. 7, the conversion of glycerol using the Pd/γ-$Al_2O_3$ catalyst for the different $H_2O_2$ concentrations employed is presented. As can be seen, the highest conversion was obtained when the $H_2O_2$ concentration was 5.0 active $O_2$ vol., which reached a value of 19.0% for the reaction time selected. After 250 min reaction, the conversion obtained was 4.7% and 1.1% with $H_2O_2$ of 2.5 and 10.0 active $O_2$ vol., respectively. In the case of the lowest concentration of $H_2O_2$ used, the result may be a consequence of an insufficient amount of $O_2$ available for the oxidation reaction. On the other hand, it is well known that the platinum group metal catalysts have a marked tendency to be poisoned by oxygen, either by simple blocking of the adsorption sites or by the migration of adsorbed oxygen atoms into the Pt lattice [28]. The formation of chemisorbed atomic oxygen from hydrogen peroxide used as the oxidizing agent can be explained by

$$H_2O_2 \rightarrow H_2O + 1/2\ O_2$$
$$O_2 + 2\ * \rightarrow 2O\ *$$

where * is an adsorption active site. Hydrogen peroxide releases oxygen during decomposition, which under the experimental conditions in which the catalytic oxidation reaction was carried out (20–80 °C) adsorbs dissociatively on Pt either reversibly or irreversibly [29]. Oxygen adsorption decreases the probability of organic substrate adsorption, which accounted

**Table 2**
XPS results of the binding energies of the Al 2*p*, O 1*s*, Pd $3d_{5/2}$ and Pb $4f_{7/2}$ levels and surface ratios of Pd/Al and Pb/Al obtained from the deconvolution of the XPS spectra.

| Catalyst | BE (eV) | | | | Pd/Al (at) | Pb/Al (at) |
|---|---|---|---|---|---|---|
| | Al 2*p* | O 1*s* | Pd $3d_{5/2}$ | Pb $4f_{7/2}$ | | |
| Pd/γ-$Al_2O_3$ | 74.5 | 531.6 | 335.0 | — | 0.0037 | — |
| PdPb0.25 | 74.5 | 531.5 | 335.2 | 136.7 (27)<br>139.2 (73) | 0.0051 | 0.0081 |
| PdPb0.50 | 74.5 | 531.6 | 335.2 | 136.6 (22)<br>139.2 (78) | 0.0040 | 0.0133 |
| PdPb1.00 | 74.5 | 531.5 | 335.2 | 136.6 (28)<br>139.2 (72) | 0.0048 | 0.0245 |
| PdPb1.60 | 74.5 | 531.5 | 335.2 | 136.7 (24)<br>139.3 (76) | 0.0047 | 0.0331 |

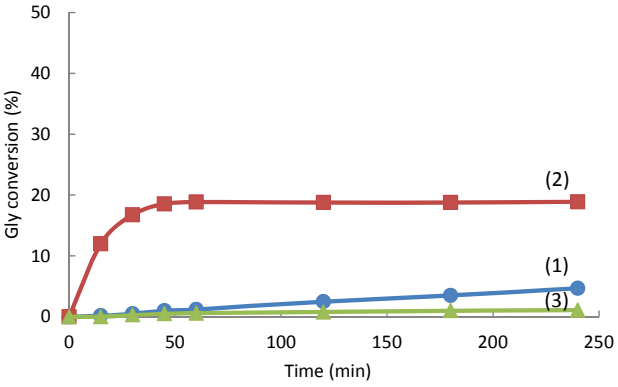


**Fig. 7.** Conversion of glycerol as a function of time for Pd/γ-$Al_2O_3$ catalyst using different $H_2O_2$ concentrations. (1) 2.5 active $O_2$ vol.; (2) 5.0 active $O_2$ vol.; (3) 10.0 active $O_2$ vol. Reaction conditions: glycerol (0.3 mol/L), catalyst (0.1 g), pH = 11, 45 °C, 500 r/min, 4 h.

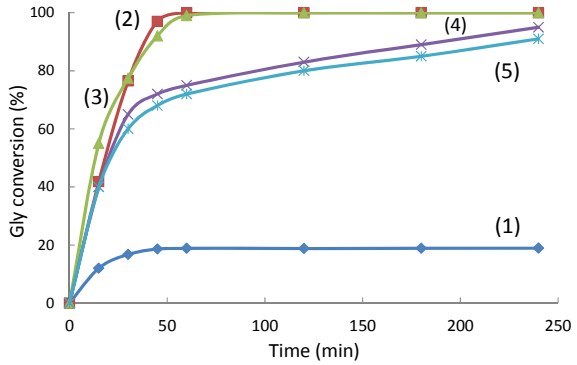


**Fig. 8.** Conversion of glycerol as a function of time for Pd/γ-$Al_2O_3$ (1), PdPb0.25 (2), PdPb0.5 (3), PdPb1.00 (4), and PdPb1.60 (5) catalysts. Reaction conditions: glycerol (0.3 mol/L), catalyst (0.1 g), $H_2O_2$ with 5.0 active $O_2$ vol., pH = 11, 45 °C, 500 r/min, 4 h.

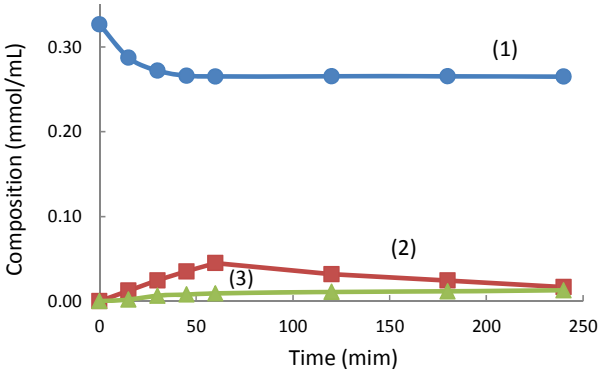


**Fig. 9.** Composition of GLY (1), GLyA (2) and GLyCA (3) versus reaction time over Pd/γ-$Al_2O_3$ catalyst. Reaction conditions: glycerol (0.3 mol/L) catalyst (0.1 g), $H_2O_2$ with 5.0 active $O_2$ vol., pH = 11, 45 °C, 500 r/min, 4 h.

for the low activity of Pd/γ-$Al_2O_3$ in glycerol oxidation. Taking into account these results, the rest of the tests were performed with $H_2O_2$ having a concentration of 5.0 active $O_2$ vol.

Fig. 8 shows the glycerol conversion obtained with the different catalysts. The results shown in this figure corresponded to the reaction conditions described in the experimental section. As mentioned, the glycerol conversion obtained with the monometallic Pd/γ-$Al_2O_3$ catalyst (Fig. 8) was 19.0% at the end of the reaction.

Palladium-lead catalysts were also tested. The results are depicted in Fig. 8. Glycerol conversion increased with the addition of Pb: PdPb0.25 and PdPb0.50 catalysts yielded 100% conversion at the end of the reaction, whereas PdPb1.00 and PdPb1.60 catalysts gave 95% and 91% conversion, respectively, at the end of the reaction.

Table 3 lists the initial rates (measured at 10% conversion) obtained with Pd/γ-$Al_2O_3$ and the four bimetallic catalysts. It can be seen that initially, the addition of Pb increased the reaction rate from 0.041 mol Gly $s^{-1}$ $g_{Pd}^{-1}$ for Pd/γ-$Al_2O_3$ to 0.142 and 0.185 mol Gly $s^{-1}$ $g_{Pd}^{-1}$ for PdPb0.25 and PdPb0.50 catalysts, respectively. A further increase in the lead content decreased the reaction rate to 0.138 mol Gly $s^{-1}$ $g_{Pd}^{-1}$ for the two catalysts with the higher lead contents (PdPb1.00 and PdPb1.60). This "volcanic" behavior can be attributed to the fact that up to a certain concentration, Pb caused an isolation effect on the active sites of Pd (most likely separated by "islands" of PdPb alloy, according to the XPS results). However, a higher amount of Pb led to a substantial coverage of the surface Pd atoms and decreased the number of active sites for the reaction. Analogous results have been reported in the literature for a series of bimetallic Pt-Bi catalysts supported on active carbon, which were used for glycerol oxidation with oxygen under atmospheric pressure [30].

Regarding selectivity, the monometallic catalyst yielded 73% of GlyA and 15% of GlyCA at the maximum conversion achieved (19%). In the liquid phase, no other reaction products were detected, indicating that the difference from 100% was due to the formation of gas products, which were not analyzed. This was a very likely result because Pd catalysts are highly active in the oxidation of these compounds to $CO_2$, as reported by Gallezot et al. [31], for instance. These authors analyzed the behavior of a 5 wt% Pd/C catalyst in the oxidation of glycerol with air as a function of pH. An increase in pH from 7 to 9 and 11 increased the selectivity to GlyA from 30% to 55% and 77%, respectively. This last value was very similar to the one obtained in the present paper, with $H_2O_2$ as oxidant and working at a pH of 11. The selectivity obtained with Pd/γ-$Al_2O_3$ can be explained by considering that glycerol was oxidized first at the primary hydroxy group of glycerol giving GlyHD (not observed), and it continued its oxidation to GlyA. This latter product was slowly oxidized to give GlyCA, probably through the formation of tartronic acid (not observed) [32]. In Fig. 9, the variation of the composition of glycerol and its oxidation products as a function of time is presented. These results agreed with those reported in the literature, where monometallic Pd catalysts promoted the oxidation of the primary hydroxy group

**Table 3**
Initial reaction rates of the catalysts determined at 10% conversion.

| Catalyst | $r_i$ (mol Gly $s^{-1}$ $g_{Pd}^{-1}$) |
|---|---|
| Pd/γ-$Al_2O_3$ | 0.041 |
| PdPb0.25 | 0.142 |
| PdPb0.50 | 0.185 |
| PdPb1.00 | 0.138 |
| PdPb1.60 | 0.138 |

Reaction conditions: glycerol (0.3 mol/L), catalyst (0.1 g), $H_2O_2$ with 5.0 active $O_2$ vol., pH = 11, 45 °C, 500 r/min, 4 h.

**Table 4**
Oxidation of glycerol using alumina supported bimetallic PdPb catalysts.

| Catalyst | Conversion [a] (%) | Selectivity [b] (%) | | | | |
|---|---|---|---|---|---|---|
| | | DIHA | GlyA | GlyCA | GlyHD | Others |
| PdPb0.25 | 100.0 | 59.0 | 12.0 | 25.0 | 2.0 | 2.0 |
| PdPb0.5 | 100.0 | 58.0 | 33.0 | 7.8 | — | 1.2 |
| PdPb1.00 | 95.0 | 34.0 | 36.2 | 16.0 | — | 13.8 |
| PdPb1.60 | 91.0 | 25.0 | 47.0 | 16.0 | — | 12.0 |

[a] Maximum conversion reached after 4 h reaction.
[b] Selectivity at 85% conversion.
Reaction conditions: glycerol (0.3 mol/L), catalysts (0.1 g), $H_2O_2$ with 5.0 active $O_2$ vol., pH = 11, 45 °C, 500 r/min, 4 h.

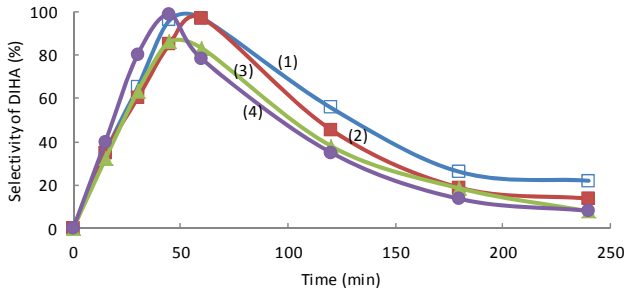


**Fig. 10.** Selectivity to DIHA as a function of time for different catalysts. (1) PdPb0.25; (2) PdPb0.50; (3) PdPb1.00; (4) PdPb1.60. Reaction conditions: glycerol (0.3 mol/L), catalyst (0.1 g), $H_2O_2$ with 5.0 active $O_2$ vol., pH = 11, 45 °C, 500 r/min, 4 h.

of glycerol to give glyceric acid [33].

The four bimetallic PdPb/γ-$Al_2O_3$ catalysts were able to oxidize glycerol to dihydroxyacetone (DIHA). At 85% conversion, the selectivity to DIHA reached 59%, 58%, 34% and 25% for PdPb0.25, PdPb0.5, PdPb1.00 and PdPb1.60 catalysts, respectively (Table 4). The time course of DIHA selectivity of the reaction over these catalysts is compared in Fig. 10. Between 45 and 60 min, the selectivity to DIHA reached values between 86% and 98.6% for the different bimetallic catalysts, but then it dropped continuously, confirming that it is a primary reaction product. These results indicated that the addition of Pb modified the regioselectivity of the reaction, and led to the preferential oxidation of the secondary hydroxy group of glycerol.

For all the bimetallic catalysts, the other major oxidation products observed were GlyA and GlyCA. According to Scheme 1, these two products were derived from the oxidation of GlyHD. This is consistent with the fact that the equilibrium DIHA↔GlyHD is strongly shifted towards GlyHD. These results have the same trend as those found by Liang et al. [34]. In Table 4, it can also be noted that with increasing Pb content, the selectivity to GlyA increased, this being the main product at 85% conversion. Simultaneously, when the lead content was increased, the selectivity to DIHA decreased. Taking into account the XPS results, this could be assigned to the fact that on the PdPb surface alloy, DIHA adsorption was weakened, favoring its subsequent transformation. Furthermore, as mentioned above, an excess amount of Pb added led to its coverage of Pd surface atoms, decreasing the number of active sites for the reaction and resulting in a lower conversion of Gly. Finally, GlyHD formation was only observed for the catalyst containing the lowest Pb content, and only 45 min after the reaction started.

## 4. Conclusions

The activity of a monometallic Pd/γ-$Al_2O_3$ catalyst for liquid phase glycerol oxidation using $H_2O_2$ as oxidizing agent was greatly improved when it was modified with lead. Depending on the Pd/Pb ratio, it was possible to convert 100% glycerol in less than 100 min. PdPb0.50 was the most selective for the production of DIHA from glycerol, reaching 59% at 100% conversion of glycerol. This performance was attributed to the close interaction between palladium and lead, as detected by TPR and XPS.

## References

[1] C. H. Zhou, J. N. Beltramini, Y. X. Fan, G. Q. Lu, *Chem. Soc. Rev.*, **2008**, 37, 527–549.
[2] C. Len, R. Luque, *Sustain. Chem. Proc.*, **2014**, 2: 1.
[3] A. Behr, J. Eilting, K. Irawadi, J. Leschinski, F. Lindner, *Green Chem.*, **2008**, 10, 13–30.
[4] R. F. Stockel, US Patent 086 977 A1, **2007**.
[5] S. K. Gupta, US Patent 092 461 A1, **2007**.
[6] A. H. Rau, H. R. Renker, N. M. Quinn, US Patent 0003 675 A1, **2007**.
[7] T. Nikaido, Y. Kobayashi, Japanese Patent 01168292 A, **1989**.

**Graphical Abstract**

*Chin. J. Catal.*, 2016, 37: 1982–1990 doi: 10.1016/S1872-2067(16)62531-7

**Oxidation of glycerol with $H_2O_2$ on Pb-promoted Pd/γ-$Al_2O_3$ catalysts**

María L. Faroppa, Juan J. Musci, María E. Chiosso, Claudia G. Caggiano, Hernán P. Bideberripe, José L. García Fierro, Guillermo J. Siri, Mónica L. Casella*
*National University of Northwestern Buenos Aires, Argentina; National University of La Plata, Argentina; Institute of Catalysis and Petrochemistry, CSIC, Spain*

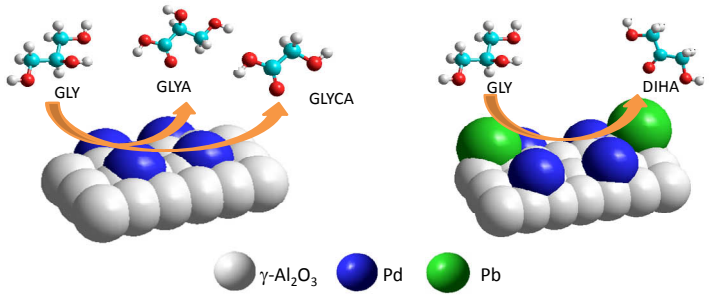


Over bimetallic PdPb catalysts, glycerol is selectively oxidized towards dihydroxyacetone whith $H_2O_2$ as oxidizing agent.

[8] T. Imanaka, H. Terasaki, A. Fujio, Y. Yokota, Japanese Patent 05331100 A, **1993**.
[9] S. Gil, M. Marchena, C. M. Fernández, L. Sánchez-Silva, A. Romero, J. L. Valverde, *Appl. Catal. A*, **2013**, 450, 189–203.
[10] B. T. Kusema, D. Y. Murzin, *Catal. Sci. Technol.*, **2013**, 3, 297–307.
[11] N. Dimitratos, J. A. López-Sánchez, G. J. Hutchings, *Chem. Sci.*, **2012**, 3, 20–44.
[12] C. P. Vinod, K. Wilson, A. F. Lee, *J. Chem. Technol. Biotechnol.*, **2011**, 86, 161–171.
[13] H. Wang, W. B. Fan, Y. He, J. G. Wang, J. N. Kondo, T. Tatsumi, *J. Catal.*, **2013**, 299, 10–19.
[14] F. Porta, L. Prati, *J. Catal.*, **2004**, 224, 397–403.
[15] N. Dimitratos, C. Messi, F. Porta, L. Prati, A. Villa, *J. Mol. Catal. A*, **2006**, 256, 21–28.
[16] S. Carrettin, P. McMorn, P. Johnston, K. Griffin, C. J. Kielyc, G. J. Hutchings, *Phys. Chem. Chem. Phys.*, **2003**, 5, 1329–1336.
[17] W. C. Ketchie, Y. L. Fang, M. S. Wong, M. Murayama, R. J. Davis, *J. Catal.*, **2007**, 250, 94–101.
[18] M. Wenkin, P. Ruiz, B. Delmon, M. Devillers, *J. Mol. Catal. A*, **2002**, 180, 141–159.
[19] C. Keresszegi, T. Mallat, J. D. Grunwaldt, A. Baiker, *J. Catal.*, **2004**, 225, 138–146.
[20] M. S. Gross, B. S. Sánchez, C. A. Querini, *Appl. Catal. A*, **2015**, 501, 1–9.
[21] V. H. Sandoval, C. E. Gigola, *Appl. Catal. A*, **1996**, 148, 81–96.
[22] P. C. Aben, *J. Catal.*, **1968**, 10, 224–229.
[23] M. B. Fernández, C. M. Piqueras, G. M. Tonetto, G. Crapiste, D. E. Damiani, *J. Mol. Catal. A*, **2005**, 233, 133–139.
[24] J. Goetz, M. A. Volpe, A. M. Sica, C. E. Gigola, R. Touroude, *J. Catal.*, **1997**, 167, 314–323.
[25] G. Beketov, B. Heinrichs, J. P. Pirard, S. Chenakin, N. Kruse, *Appl. Surf. Sci.*, **2013**, 287, 293–298.
[26] J. C. Bertolini, P. Delichere, B. C. Khanra, J. Massardier, C. Noupa, B. Tardy, *Catal. Lett.*, **1990**, 6, 215–223.
[27] B. S. Sánchez, M. S. Gross, N. C. Insaurralde, A. Palmero, C. A. Querini, in: Proceedings of the XVIII Congreso Argentino de Catálisis, Nueva Editorial Universitaria (UNSL), San Luis, **2013**, 1–8.
[28] H. E. Van Dam, L. J. Wisse, H. Van Bekkum, *Appl. Catal.*, **1990**, 61, 187–197.
[29] V. R. Gangwal, J. Van der Shaaf, B. F. M. Kuster, J. C. Schouten, *J. Catal.*, **2005**, 229, 389–403.
[30] D. Liang, S. Y. Cui, J. Gao, J. H. Wang, P. Chen, Z. Y. Hou, *Chin. J. Catal.*, **2011**, 32, 1831–1837.
[31] R. Garcia, M. Besson, P. Gallezot, *Appl. Catal. A*, **1995**, 127, 165–176.
[32] S. Demirel, K. Lehnert, M. Lucas, P. Claus, *Appl. Catal. B*, **2007**, 70, 637–643.
[33] H. Kimura, K. Tsuto, T. Wakisawa, Y. Kazumi, Y. Inaya, *Appl. Catal. A*, **1993**, 96, 217–228.
[34] D. Liang, J. Gao, J. H. Wang, P. Chen, Y. F. Wei, Z. Y. Hou, *Catal. Commun.*, **2011**, 12, 1059–1062.